Finite Element Modelling and Design of Welded Stainless Steel I-section Columns

Yidu Bu and Leroy Gardner

Imperial College London, UK

Abstract

Stainless steel is widely used in construction due to its combination of excellent mechanical properties, durability and aesthetics. Towards more sustainable infrastructure, stainless steel is expected be more commonly specified and to feature in more substantial structural applications in the future; this will require larger and typically welded cross-sections. While the structural response of cold-formed stainless steel sections has been extensively studied in the literature, welded sections have received less attention to date. The stability and design of conventionally welded and laser-welded austenitic stainless steel compression members are therefore the focus of the present research. Finite element (FE) models were developed and validated against a total of 59 experiments, covering both conventionally welded and laser-welded columns, for which different residual stress patterns were applied. A subsequent parametric study was carried out, considering a range of cross-section and member geometries. The existing experimental results, together with the numerical data generated herein, were then used to assess the buckling curves given in European, North American and Chinese design standards. Following examination of the data and reliability analysis, new buckling curves were proposed, providing, for the first time, design guidance for laser-welded stainless steel members.

Keywords

Columns, Compression members, Eurocode 3, Finite element modelling, Flexural buckling, Laser-welding, Numerical modelling, Residual stress, Stainless steel

1 Introduction

Stainless steel is used in a wide range of applications within the construction industry. To date, the predominant product types have been cold-formed sections, whose structural behaviour have been the most extensively explored in research and whose design have the broadest coverage in international structural design standards. In recent years, however, welded stainless steel sections, offering larger cross-section sizes and higher load-bearing capacities, have become more widely studied and employed in practice.

In conventional welding processes, two pieces of material are joined together by melting the base metal and an additional filler material. Some of the most commonly used welding methods include shielded metal arc welding (SMAW), gas tungsten arc welding (GTAW) and gas metal arc welding (GMAW). An innovative alternative fabrication process is laser-welding, which uses laser beams to locally melt and join two pieces of metal with minimum heat input, producing smaller heat affected zones, lower thermal distortions and lower residual stresses than would typically arise from traditional welding processes. Laser-welded I-section columns may, due to the lower residual stress magnitudes, show superior structural performance over their conventionally welded counterparts, and exploration of this point is a key aspect of the paper.

The structural behaviour of welded stainless steel compression members has been studied for I-sections [1-4] and box sections [5, 6]. The key experimental results from these studies are employed herein for the validation of finite element models for both conventionally welded [1, 2] and laser-welded [3] stainless steel I-section columns. The validated numerical models are used to generate a series of parametric data and the combined set of experimental and numerical results are employed to assess the design provisions in EN 1993-1-4 [7], Design Guide 27 [8], and CECS-410 [9] for stainless steel compression members.

2 Finite Element Modelling

2.1 Introduction

A numerical investigation on welded stainless steel I-section columns was carried out using the general-propose finite element (FE) package ABAQUS. The models were validated against the experimental results from previous studies on the flexural buckling of welded stainless steel I-section columns [1-3]. For conventionally welded members, Burgan et al. [1] carried out 15 tests on I-section columns of austenitic grade EN 1.4301 and duplex grade EN 1.4462 stainless steel, with 6 buckling about the minor axis and 9 buckling about the major axis, while Yang et al. [2] performed 22 tests on I-section columns of austenitic grade EN 1.4301 and duplex grade EN 1.4462 stainless steel, with 12 buckling about the minor axis and 10 buckling about the major axis. For laser-welded members, Gardner et al. [3] conducted 22 tests on I-section columns of austenitic grades EN 1.4307, 1.4571 and 1.4404 stainless steel, with 14 buckling about the minor axis and 8 buckling about the major axis. The section sizes, stainless steel grades, axis of buckling and method of fabrication

Presented by Yidu Bu - y.bu13@imperial.ac.uk

of these test specimens are summarised in Table 1, where L is the buckling length of the columns. The cross-sections (eg. I-160×80×6×10) are designated as follows: I-section height (h) × section width (b_f) × web thickness (t_w) × flange thickness (t_f). The sum of the measured global geometric imperfection magnitude plus any additional applied load eccentricity, termed the total measured eccentricity w_m, is also tabulated; such measurements were not reported in [1]. The experimental results described in [1-3], including the full load-displacement histories, ultimate loads and failure modes, were used for the validation of the numerical models developed in this paper. Upon validation of the models, a series of parametric studies was carried out to assess the structural behaviour of both conventionally welded and laser-welded I-section columns.

Table 1 Summary of geometric dimensions, material and fabrication method of the column specimens

Welding type and references	Cross-section	Specimen ID	Grade	Axis of buckling	L (mm)	h (mm)	b_f (mm)	t_w (mm)	t_f (mm)	w_m (mm)
Conventional welding Burgan et al. [1]	I-160×80×6×10	I160×80-C1	1.4301	Minor	650.0	158.00	79.50	6.00	9.80	-
	I-160×80×6×10	I160×80-C2			1248.0	161.70	80.80	6.00	9.80	-
	I-160×80×6×10	I160×80-C3			2046.0	161.40	79.80	6.00	9.80	-
	I-160×160×6×10	I160×160-C1			1248.0	158.30	159.20	6.00	9.80	-
	I-160×160×6×10	I160×160-C2			2049.0	157.70	159.90	6.00	9.90	-
	I-160×160×6×10	I160×160-C3			3347.0	158.00	160.10	6.00	9.80	-
	I-160×80×6×10	I160×80-C1	1.4301	Major	2048.0	157.00	79.40	6.00	9.80	-
	I-160×80×6×10	I160×80-C2			3343.0	157.60	78.90	6.00	9.80	-
	I-160×80×6×10	I160×80-C3			5031.0	158.50	80.10	6.00	9.80	-
	I-160×160×6×10	I160×160-C1			2025.0	158.30	160.00	6.00	9.90	-
	I-160×160×6×10	I160×160-C2			3348.0	158.40	159.80	6.00	9.90	-
	I-160×160×6×10	I160×160-C3			5145.0	158.00	159.20	6.00	9.90	-
	I-160×160×6×10	I160×160-C1	1.4462		2050.0	162.70	159.80	6.80	10.60	-
	I-160×160×6×10	I160×160-C2			3348.0	161.40	159.50	6.80	10.60	-
	I-160×160×6×10	I160×160-C3			5046.0	160.40	161.00	6.80	10.60	-
Conventional welding Yang et al. [2]	I-150×150×6×10	H304-1500	1.4301	Minor	1875.7	150.20	149.10	6.00	10.00	2.42
	I-150×150×6×10	H304-2000			2377.4	150.10	149.10	6.00	10.00	17.35
	I-150×150×6×10	H304-3000			3383.7	150.00	149.60	6.00	10.00	4.10
	I-150×150×6×10	H304-3500			3877.3	149.60	149.60	6.00	10.00	32.86
	I-150×150×6×10	H304-4000			4376.8	150.00	149.40	6.00	10.00	26.85
	I-150×120×6×10	H304-4000-B			4369.1	149.70	119.10	6.00	10.00	12.66
	I-150×150×6×10	H2205-1500	1.4462		1879.3	150.80	149.90	6.00	10.20	10.38
	I-150×150×6×10	H2205-2000			2378.9	150.40	150.00	6.00	10.20	5.02
	I-150×150×6×10	H2205-3000			3381.4	150.30	149.70	6.00	10.20	44.49
	I-150×150×6×10	H2205-3500			3880.8	150.10	151.20	6.00	10.20	43.12
	I-150×150×6×10	H2205-4000			4375.5	150.10	149.90	6.00	10.20	3.90
	I-150×120×6×10	H2205-4000-B			4378.2	150.30	120.10	6.00	10.20	13.77
	I-150×150×6×10	I304-2000	1.4301	Major	2377.1	149.80	149.20	6.00	10.00	8.17
	I-150×150×6×10	I304-3000			3373.5	150.30	149.30	6.00	10.00	3.64
	I-150×150×6×10	I304-3500			3874.8	110.40	149.50	6.00	10.00	5.00

	I-150×150×6×10	I304-4000			4374.4	150.20	150.00	6.00	10.00	4.02
	I-100×120×6×10	I304-4500			4872.9	100.00	120.10	6.00	10.00	0.93
	I-150×150×6×10	I2205-2000			2380.2	150.30	150.70	6.00	10.20	10.17
	I-150×150×6×10	I2205-3000			3377.2	150.00	149.90	6.00	10.20	3.68
	I-150×150×6×10	I2205-3500	1.4462		3883.7	150.40	150.90	6.00	10.20	1.36
	I-150×150×6×10	I2205-4000			4378.7	150.10	148.50	6.00	10.20	0.53
	I-110×150×6×10	I2205-4500			4876.0	110.80	150.40	6.00	10.20	0.93
Laser-welding Gardner et al. [3]	I-140×140×10×12	1A1			1030.1	139.73	140.64	9.73	11.88	0.35
	I-140×140×10×12	1A2			2032.1	140.12	140.62	9.86	11.91	1.42
	I-50×50×4×4	2A1	1.4307		1631.1	50.43	50.53	4.03	4.05	0.53
	I-50×50×4×4	2A2			1931.1	50.68	50.54	4.00	4.02	1.52
	I-160×82×10×12	3A1			1730.1	160.86	83.23	9.88	11.84	1.22
	I-160×82×10×12	3A2			2323.1	160.49	82.80	9.88	11.85	1.67
	I-102×68×5×5	4A1		Minor	931.1	101.56	67.96	5.03	5.00	0.80
	I-102×68×5×5	4A2			1330.1	101.51	67.96	5.02	5.04	0.65
	I-102×68×5×5	4A3	1.4571		1730.1	101.80	67.99	5.03	5.02	1.05
	I-102×68×5×5	4A4			2030.1	101.76	67.88	4.99	4.98	1.85
	I-102×68×5×5	4A5			2430.1	101.77	67.83	5.01	4.99	1.60
	I-150×75×7×10	5A1			634.1	150.18	75.87	6.91	9.81	0.55
	I-150×75×7×10	5A2	1.4404		1181.1	150.22	75.91	6.91	9.85	1.35
	I-150×75×7×10	5A3			2331.1	151.19	75.90	6.87	9.86	1.44
	I-50×50×4×4	2B1			680.1	51.00	50.56	3.99	3.93	1.05
	I-50×50×4×4	2B2			1130.1	50.59	50.60	4.04	3.86	1.90
	I-50×50×4×4	2B3	1.4307		1580.1	50.28	50.32	3.99	3.98	2.15
	I-50×50×4×4	2B4		Major	2530.1	50.90	50.55	4.01	3.94	3.00
	I-50×50×4×4	2B5			3030.1	50.21	50.55	4.00	3.91	3.40
	I-102×68×5×5	4B1			1330.1	101.91	67.51	4.99	4.94	1.05
	I-102×68×5×5	4B2	1.4571		2330.1	102.37	67.94	5.21	5.01	3.15
	I-102×68×5×5	4B3			3080.1	102.11	67.93	5.04	5.01	3.90

2.2 Basic modelling assumptions

The four-noded shell element with reduced integration (S4R) from the ABAQUS element library was adopted to simulate the I-section columns. This element type has been shown to be suitable for the modelling of similar members in previous studies [5, 10]. For the validation of the FE models, the measured geometric and material properties of the corresponding test specimens were employed. The measured engineering stress-strain responses were first represented using the two-stage modified Ramberg-Osgood model [11-14], then converted into true stress σ_{true} and log plastic strain ε_{ln}^{pl} using Equations (1) and (2), where σ_{nom} and ε_{nom} are the engineering stress and strain and E is the Young's modulus, and finally input into ABAQUS in multi-linear form with 50 intervals. Note that for the replication of the test series by Gardner et al. [3], compressive material properties were adopted and the conversion from the measured engineering stress-strain curves to the true stress-strain curves utilised Equations (1) and (2), but with the $(1+\varepsilon_{nom})$ term changed to $(1-\varepsilon_{nom})$, assuming absolute values of strain are used. Alternatively, compressive strains can be input into Equations (1) and (2) as negative values.

$$\sigma_{true} = \sigma_{nom}(1+\varepsilon_{nom}) \,, \tag{1}$$

$$\varepsilon_{\ln}^{pl} = \ln(1+\varepsilon_{nom}) - \frac{\sigma_{true}}{E}. \quad (2)$$

In accordance with the test setups in [1–3], boundary conditions were applied to simulate pin-ended conditions; thus all degrees of freedom at the two end cross-sections of the columns, except vertical translation at the loaded end and rotation about the axis of buckling at both ends, were restrained. For columns buckling about the major axis, out-of-plane deflections were also restrained at the web-to-flange junctions to replicate the lateral restraints used in the tests.

2.3 Initial geometric imperfections

Initial geometric imperfections were also incorporated into the numerical models. Following the approach adopted in previous studies [15, 16], an elastic buckling analysis was firstly carried out to determine the lowest global and local eigenmodes. These buckling mode shapes were then assigned to the models to represent the initial geometric imperfection. Since measurements of local imperfections were not reported in [1, 2], their amplitude was taken as the values $w_{D\&W}$ predicted by the modified Dawson and Walker (D&W) model [17, 18], as given by Equation (3).

$$w_{D\&W} = 0.023\left(\frac{f_y}{f_{cr,min}}\right)t, \quad (3)$$

where $f_{cr,min}$ is the minimum elastic buckling stress of all the plate elements making up the cross-section, f_y is the yield (0.2% proof) stress and t is the thickness of the plate element. The amplitude of the global imperfection was taken as the measured value, where available, and $L/1000$ in the validation study (see Section 2.5) and $L/1000$ throughout the subsequent parametric studies (see Section 2.6). A geometrically and materially nonlinear analysis was then performed using the modified Riks method [19, 20], allowing the full load-deformation response of the columns including the unloading path to be traced.

2.4 Residual stress pattern

A number of studies have been carried out to investigate the residual stress distributions in welded stainless steel sections [21–25]. Based on experimental measurements, predictive models have been proposed for both conventionally welded [25] and laser-welded [3] I-sections, with the latter having lower magnitudes due to the reduced heat input during fabrication. The residual stress distribution patterns proposed in [25] and [3] were adopted in the numerical models for conventionally welded and laser-welded cross-sections, respectively. The key parameters for the residual stress patterns for stainless steel I-sections are set out, with reference to Fig. 1 for the definition of the symbols, in Table 2. Values of the corresponding parameters for conventionally welded carbon steel [26, 27] I-sections are also shown for comparison purposes.

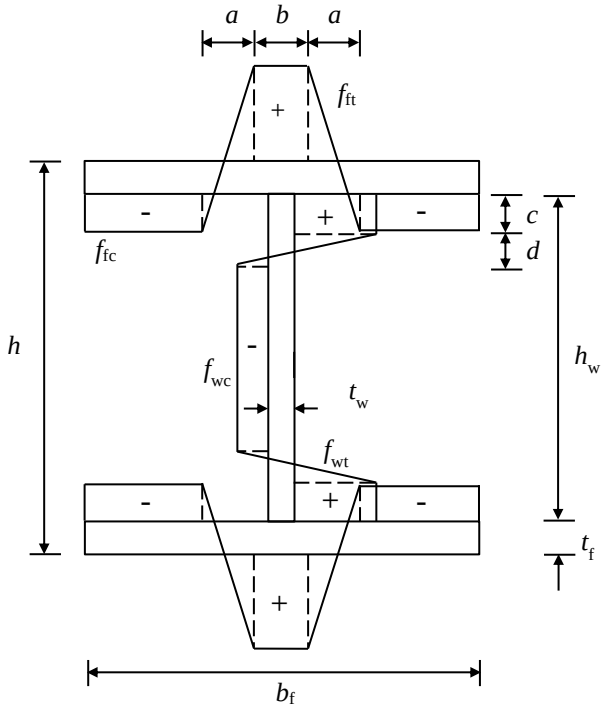

Fig. 1 General residual stress distribution for welded I-sections (+ve=tension;-ve=compression)

Table 2 Parameters in residual stress predictive models for welded I-sections

Predictive model	Material and welding method	$f_{ft} = f_{wt}$	$f_{fc} = f_{wc}$	a	b	c	d
Yuan et al. [25]	Conventionally welded austenitic stainless steel	$0.8f_y$	From equilibrium	$0.225b_f$	$0.05b_f$	$0.025h_w$	$0.225h_w$
Yuan et al. [25]	Conventionally welded duplex stainless steel	$0.6f_y$	From equilibrium	$0.225b_f$	$0.05b_f$	$0.025h_w$	$0.225h_w$
Gardner et al.[3]	Laser-welded austenitic stainless steel	$0.5f_y$	From equilibrium	$0.1b_f$	$0.075b_f$	$0.025h_w$	$0.05h_w$
ECCS [26]	Conventionally welded carbon steel	f_y	$0.25f_y$	$0.05b_f$	$0.15b_f$	$0.075h_w$	$0.05h_w$
BSK 99 [27]	Conventionally welded carbon steel	$0.5f_y$	From equilibrium	$0.75t_f$	$1.5t_f$	$1.5t_w$	$1.5t_w$

2.5 Validation of models

The FE models were validated against the experimental results from the aforementioned studies [1–3] on welded stainless steel columns. The measured geometric and material properties, as reported in the original studies, were used in the numerical models. Four combinations of geometric imperfection amplitudes and residual stress were considered: (a) Combination 1: measured global imperfection amplitude w_m, local imperfection amplitude from Equation (3) $w_{D\&W}$ and residual stresses from Section 2.4, (b) Combination 2: measured global imperfection amplitude w_m and local imperfection amplitude from Equation (3) $w_{D\&W}$, (c) Combination 3: global imperfection amplitude of $L/1000$, local imperfection amplitude from Equation (3) $w_{D\&W}$ and residual stresses from Section 2.4, (d) Combination 4: global imperfection amplitude of $L/1000$ and local imperfection amplitude from Equation (3) $w_{D\&W}$. The residual stress patterns described in Section 2.4 were assigned to the FE models according to the material type and the fabrication process of the columns.

The numerical results, including the ultimate loads, the load-lateral deflection responses and the failure modes were compared with the experimental results. The ratios of the ultimate loads obtained from the laboratory tests N_{test} to the ultimate loads obtained from the FE models N_{FE} are shown in Table 3, considering the four different combinations of geometric imperfections and residual stresses (denoted as 'RS' in the table). For the experimental results reported in [1], only combinations (c) and (d) are considered since measurements of imperfections were not reported. The mean values and the coefficients of variation (COV) of the N_{test}/N_{FE} ratios for the conventionally welded specimens, the laser-welded specimens and all specimens are presented in the table. The best agreement between the test and FE results would be anticipated for Combination 1, where the measured global imperfections and residual stresses were included. However, while this was generally the case for the test series by Gardner et al. [3], it was not the case for the experiments of Yang et al. [2]. In fact, some test specimens were reported to have very large measured imperfections and adoption of these values in the FE models led to very low FE resistance predictions. Significantly improved resistance predictions were achieved using the constant imperfection amplitude of $L/1000$ (i.e. Combination 3). It is therefore asserted that there might have been errors in the geometric imperfection measurements.

Table 3 Comparison of experimental and numerical results

Welding type and references	Cross-section	Specimen ID	Axis of buckling	Geometric imperfection and residual stress combination			
				$w_m+w_{D\&W}$+RS N_{test}/N_{FE}	$w_m+w_{D\&W}$ N_{test}/N_{FE}	$L/1000+w_{D\&W}$+RS N_{test}/N_{FE}	$L/1000+w_{D\&W}$ N_{test}/N_{FE}
Conventional welding Burgan	I-160×80×6×10	I160×80-C1		-	-	0.94	0.93
	I-160×80×6×10	I160×80-C2	Minor	-	-	0.98	0.88
	I-160×80×6×10	I160×80-C3		-	-	1.20	0.99

et al. [1]	I-160×160×6×10	I160×160-C1		-	-	0.84	0.95
	I-160×160×6×10	I160×160-C2		-	-	0.80	0.79
	I-160×160×6×10	I160×160-C3		-	-	0.98	0.90
	I-160×80×6×10	I160×80-C1		-	-	0.99	0.99
	I-160×80×6×10	I160×80-C2		-	-	0.98	1.01
	I-160×80×6×10	I160×80-C3		-	-	0.98	0.98
	I-160×160×6×10	I160×160-C1		-	-	0.99	1.00
	I-160×160×6×10	I160×160-C2	Major	-	-	0.98	0.95
	I-160×160×6×10	I160×160-C3		-	-	1.04	1.04
	I-160×160×6×10	I160×160-C1		-	-	0.86	0.90
	I-160×160×6×10	I160×160-C2		-	-	0.91	0.93
	I-160×160×6×10	I160×160-C3		-	-	0.92	0.90
Conventional welding Yang et al. [2]	I-150×150×6×10	H304-1500		1.21	1.14	1.08	1.02
	I-150×150×6×10	H304-2000		1.48	1.35	1.14	1.03
	I-150×150×6×10	H304-3000		1.27	1.05	1.23	1.02
	I-150×150×6×10	H304-3500		1.77	1.58	1.20	0.98
	I-150×150×6×10	H304-4000		1.55	1.36	1.13	0.93
	I-150×120×6×10	H304-4000-B	Minor	1.49	1.27	1.29	1.08
	I-150×150×6×10	H2205-1500		1.30	1.17	1.08	0.98
	I-150×150×6×10	H2205-2000		1.17	1.01	1.07	0.93
	I-150×150×6×10	H2205-3000		1.86	1.73	1.12	0.98
	I-150×150×6×10	H2205-3500		1.96	1.82	1.24	1.11
	I-150×150×6×10	H2205-4000		1.16	1.06	1.17	1.06
	I-150×120×6×10	H2205-4000-B		1.56	1.41	1.31	1.23
	I-150×150×6×10	I304-2000		0.93	0.95	0.95	0.97
	I-150×150×6×10	I304-3000		1.05	1.07	1.03	1.06
	I-150×150×6×10	I304-3500		0.76	0.77	0.75	0.76
	I-150×150×6×10	I304-4000		0.92	0.92	0.94	0.94
	I-100×120×6×10	I304-4500	Major	0.87	0.78	0.94	0.86
	I-150×150×6×10	I2205-2000		1.09	1.09	0.95	0.97
	I-150×150×6×10	I2205-3000		0.99	0.98	0.97	0.97
	I-150×150×6×10	I2205-3500		0.95	0.92	1.00	0.91
	I-150×150×6×10	I2205-4000		0.92	0.87	1.00	0.95
	I-110×150×6×10	I2205-4500		1.07	1.02	1.16	1.10
Mean for conventionally welded specimens				1.24	1.15	1.03	0.97
COV for conventionally welded specimens				0.27	0.25	0.13	0.09
Laser-welding Gardner et al. [3]	I-140×140×10×12	1A1		0.98	0.97	0.98	0.97
	I-140×140×10×12	1A2	Minor	0.96	0.91	0.98	0.93
	I-50×50×4×4	2A1		0.96	0.92	1.07	1.02

I-50×50×4×4	2A2		0.85	0.82	0.90	0.86
I-160×82×10×12	3A1		0.90	0.84	0.94	0.89
I-160×82×10×12	3A2		0.89	0.86	0.93	0.90
I-102×68×5×5	4A1		1.03	1.00	1.03	1.00
I-102×68×5×5	4A2		1.00	0.94	1.07	1.01
I-102×68×5×5	4A3		0.98	0.94	1.04	1.00
I-102×68×5×5	4A4		0.98	0.94	1.00	0.96
I-102×68×5×5	4A5		0.99	0.96	1.05	1.01
I-150×75×7×10	5A1		1.00	0.99	1.00	0.99
I-150×75×7×10	5A2		0.98	0.94	0.97	0.93
I-150×75×7×10	5A3		0.95	0.89	1.00	0.94
I-50×50×4×4	2B1	Major	1.03	1.03	1.06	1.06
I-50×50×4×4	2B2		1.01	1.01	1.02	1.02
I-50×50×4×4	2B3		1.01	1.00	1.01	1.01
I-50×50×4×4	2B4		1.03	1.01	1.01	0.99
I-50×50×4×4	2B5		0.95	0.93	1.06	1.04
I-102×68×5×5	4B1		1.00	1.01	0.99	1.00
I-102×68×5×5	4B2		1.00	1.01	0.98	0.99
I-102×68×5×5	4B3		0.94	0.95	0.92	0.93
Mean for laser-welded specimens			0.97	0.95	1.00	0.97
COV for laser-welded specimens			0.05	0.06	0.05	0.05
Mean for all specimens			1.11	1.05	1.02	0.97
COV for all specimens			0.25	0.22	0.11	0.08

The importance of including residual stresses in the FE analyses may be assessed by comparing the results of Combination 3 (with residual stresses) and Combination 4 (without residual stresses). It may be observed that the conventionally welded members show a greater drop in capacity (5.9% on average) than the laser-welded members (2.8% on average) due to the higher residual stress magnitude, and that the residual stresses are more detrimental to the specimens buckling about the minor axis (8.1% average drop in capacities for specimens buckling about the minor axis and 0.7% average drop in capacities for specimens buckling about the major axis) due to the compressive residual stresses coinciding with the most heavily compressed region of the cross-section (i.e. the flange tips). In addition to ultimate loads, examples of typical load-deflection curves are compared in Figs. 2a and 2b, for buckling about the minor and major axis, respectively. Comparisons between the failure modes exhibited by the tested specimens and those obtained from the finite element models are shown in Figs. 3a and 3b, for buckling about the minor and major axis, respectively. Good correlation may be observed in both cases. Overall, disregarding the imperfection measurements reported in [2], the FE models may be seen to provide an accurate representation of the behaviour observed in the physical tests for both the conventionally welded and laser-welded stainless steel columns.

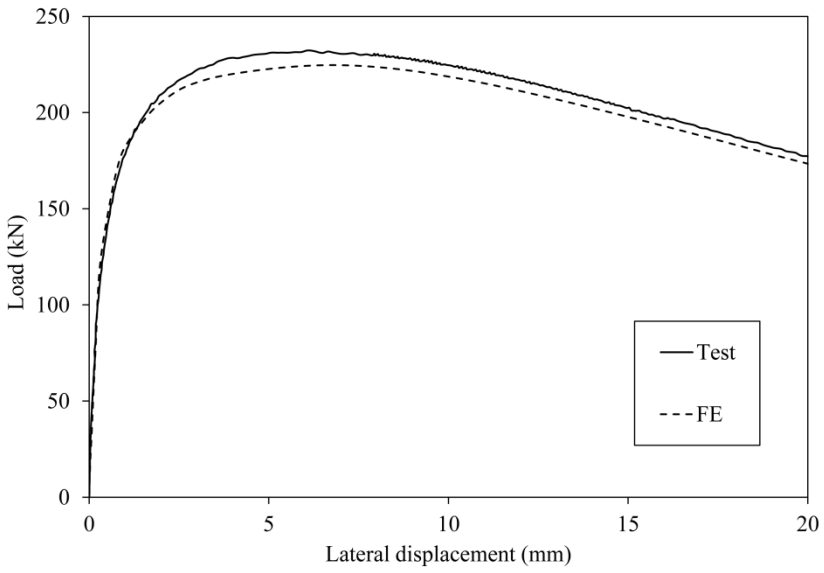

(a) Buckling about the minor axis (Specimen 4A1 tested in [3])

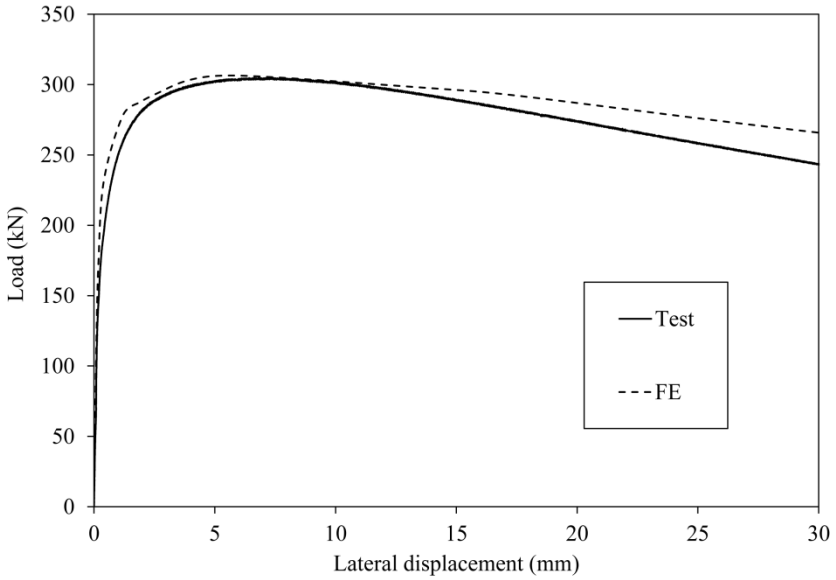

(b) Buckling about the major axis (Specimen 4B1 tested in [3])

Fig. 2 Comparison of typical test and FE load-lateral deflection curves

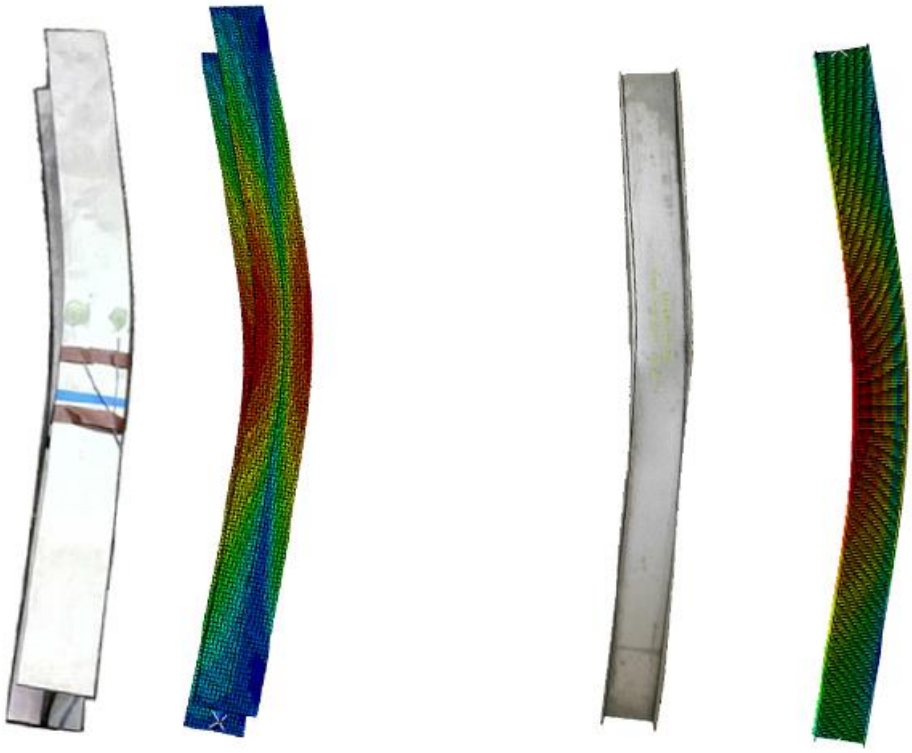

(a) Buckling about the minor axis (Specimen 4B1 tested in [3])

(b) Buckling about the major axis (Specimen 4A1 tested in [3])

Fig. 3 Comparison of typical test and FE failure modes

2.6 Parametric studies

Upon validation of the FE models, a series of parametric studies was carried out to further investigate the structural behaviour of stainless steel I-section columns. In total, 480 column models were generated, covering flexural buckling about both the minor and major axes. Throughout the parametric studies, the cross-section height was kept constant while the width of the flange was varied to give three aspect ratios *h*/*b* of 1.0, 1.5 and 2.0. The thicknesses of the flange and the web were also varied such that the non-dimensional plate slenderness of the flange $\bar{\lambda}_{p,f}$ ranged from 0.28 to 0.81, and the non-dimensional plate slenderness of the web $\bar{\lambda}_{p,w}$ ranged from 0.27 to 0.79, while for all sections, $\bar{\lambda}_{p,f} \approx \bar{\lambda}_{p,w}$. The non-dimensional plate slendernesses of the flanges and web are defined in Equations (4) and (5), respectively.

$$\bar{\lambda}_{p,f} = \sqrt{f_y / f_{cr,f}}, \tag{4}$$

$$\bar{\lambda}_{p,w} = \sqrt{f_y / f_{cr,w}}, \tag{5}$$

where $f_{cr,f}$ and $f_{cr,w}$ are the elastic buckling stresses of the outstand flanges and web, considered in isolation as in [28].

Columns of different lengths were simulated for each cross-section to give a spectrum of non-dimensional member slendernesses $\bar{\lambda}$ from 0.1 to 2.0, where $\bar{\lambda} = \sqrt{A f_y / N_{cr}}$ and Ncr is the elastic buckling load of the column. For each cross-section size and member length, FE models with residual stress patterns for both conventional welding and laser-welding were considered. The compressive stress-strain properties of the austenitic stainless steel cross-section I-102×68×5×5 tested in [3] were adopted throughout the parametric studies. For geometric imperfections and residual stresses, Combination 3 (i.e. a global imperfection amplitude of L/1000, a local imperfection amplitude given by Equation (3) and the residual stress distributions from Section 2.4) was employed throughout the parametric study. The results generated from the parametric studies, together with the experimental results, are used in the next section as the basis for assessing existing design provisions and making new design recommendations for both conventionally welded and laser-welded I-section columns.

3 Design Recommendations

The current design recommendations in the European [7], North American [8] and Chinese [9] standards for the flexural buckling of welded stainless steel I-section columns are introduced and assessed in this section.

3.1 European Standard (EC3)

In EN 1993-1-4 [7], cross-sections are grouped into 4 classes based on the slenderness of their constituent plate elements, where Class 1, 2 and 3 cross-sections are deemed to be fully-effective and capable of reaching their yield load (Af_y) under pure compression while in Class 4 (slender) cross-sections local buckling prevents attainment of the yield load. Local buckling in slender cross-sections is accounted for by using an effective area A_{eff} in place of the gross area A in the design calculations. The compressive strength (flexural buckling resistance) $N_{b,Rd}$ of a column is given by Equations (6) and (7) for columns with non-slender (Class 1-3) and slender (Class 4) cross-sections respectively:

$$N_{b,Rd} = \frac{\chi A f_y}{\gamma_{M1}}, \tag{6}$$

$$N_{b,Rd} = \frac{\chi A_{eff} f_y}{\gamma_{M1}}, \tag{7}$$

where χ is the overall buckling reduction factor and γ_{M1} is the partial safety factor.

The EC3 design approach for compression members is based on the Perry-Robertson buckling formula with an imperfection parameter $\eta = \alpha(\bar{\lambda}_{EC}-\bar{\lambda}_0)$, where α is the imperfection factor and $\bar{\lambda}_0$ is the plateau length. The Eurocode non-dimensional member slenderness is given by Equation (8).

$$\bar{\lambda}_{EC} = \sqrt{\frac{Af_y}{N_{cr}}} = \frac{L_{cr}}{i\pi}\sqrt{\frac{f_y}{E}}, \tag{8}$$

where L_{cr} is the member buckling length and i is the radius of gyration about the relevant axis. Different imperfection parameters can be used to reflect the influence of the different geometric imperfections and residual stress patterns depending on the cross-section shape, buckling axis, fabrication process and material type. The Eurocode buckling reduction factor χ_{EC} to account for member instability can be determined from Equations (9) and (10).

$$\chi_{EC} = \frac{1}{\phi + \sqrt{\phi^2 - \bar{\lambda}_{EC}^2}}, \tag{9}$$

$$\phi = 0.5\left[1+\eta+\bar{\lambda}_{EC}^2\right], \tag{10}$$

For welded stainless steel I-section columns, EN 1993-1-4 [7] adopts buckling curve 'c' (with a plateau length $\bar{\lambda}_0$=0.2 and imperfection factor α=0.49) for buckling about the major axis and curve 'd' (with a plateau length $\bar{\lambda}_0$=0.2 and imperfection factor α=0.76) for buckling about the minor axis.

3.2 North American AISC Design Guide 27

In AISC Design Guide 27 [8], the design compressive strength $N_{b,Rd}$ is given by Equation (11), where P_n is the lowest value of the flexural, torsional and flexural-torsional buckling resistance, ϕ_c is the resistance factor, F_{cr} is the buckling stress and A_g is the cross-sectional area of member.

$$N_{b,Rd} = \phi_c P_n = \phi_c F_{cr} A_g. \tag{11}$$

The buckling stress F_{cr} may be expressed in a similar manner to the Eurocode as a buckling reduction factor χ_{AISC}, given by Equations (12) and (13), multiplied by the yield stress F_y (i.e. $F_{cr} = \chi_{AISC}F_y$).

$$\chi_{AISC} = Q\left(0.50^{Q\bar{\lambda}_{AISC}^2}\right), \quad \text{for } \bar{\lambda}_{AISC}^2 \le 1.2 \tag{12}$$

$$\chi_{AISC} = \frac{0.531}{\bar{\lambda}_{AISC}^2}, \quad \text{for } \bar{\lambda}_{AISC}^2 > 1.2 \tag{13}$$

where $\bar{\lambda}^2_{\mathrm{AISC}}$ is the relative member slenderness given by Equation (14) and Q is a reduction factor for local buckling, taken equal to unity for non-slender cross-sections. Note that only a single buckling curve (Equations (12) and (13)) is provided in AISC Design Guide 27 to cover all cross-section types and buckling axes.

$$\bar{\lambda}_{\mathrm{AISC}} = \frac{KL}{\pi r}\sqrt{\frac{F_{\mathrm{y}}}{E}}, \tag{14}$$

where K is the effective length factor, L is the laterally unbraced length of the member and r is the radius of gyration.

3.3 Chinese Standard (CECS-410)

As in EC3, the design method in the Chinese Standard CECS-410 [9] for stainless steel compression members is also based on the Perry-Robertson formula. The non-dimensional member slenderness in CECS-410 $\bar{\lambda}_{\mathrm{CECS}}$ is defined in the same manner as in EC3, as given by Equation (15).

$$\bar{\lambda}_{\mathrm{CECS}} = \frac{L_{\mathrm{cr}}}{i\pi}\sqrt{\frac{f_{\mathrm{y}}}{E}}. \tag{15}$$

A set of 6 buckling curves, of the same form as EC3, are employed for different stainless steel grades, cross-sectional shapes, buckling axes and fabrication processes. The design buckling curves were derived by regression analysis to the then available stainless steel test data in China and other parts of the world. For welded stainless steel members, α=0.66 and $\bar{\lambda}_0$=0.24 are employed for buckling about the major axis and α=0.89 and $\bar{\lambda}_0$=0.26 are employed for buckling about the minor axis.

3.4 Assessment of current design methods and new proposal

In this sub-section, the experimental and numerical results for the stainless steel I-section columns are examined and compared with the current column design provisions adopted in the European, North American, and Chinese standards. The ultimate loads N_{u} from both the experiments and the numerical simulations are normalised by the yield load Af_{y} ($A_{\mathrm{eff}}f_{\mathrm{y}}$ for Class 4 cross-sections) and plotted against the non-dimensional member slenderness $\bar{\lambda}$ in Figs. 4 and 5 for flexural buckling about the minor axis and the major axis, respectively. From the figures it can be seen that all curves generally offer conservative predictions. With the AISC Design Guide only employing one buckling curve for buckling about either axes, the resistance predictions for buckling about the major axis are particularly conservative. The accuracy of each method is evaluated by means of the ratio of the test and FE ultimate loads N_{u} to predicted ultimate loads for each method ($N_{\mathrm{u}}/N_{\mathrm{EC3}}$, $N_{\mathrm{u}}/N_{\mathrm{AISC}}$ and $N_{\mathrm{u}}/N_{\mathrm{CECS}}$) in Table 4. Note that all comparisons were made based on the measured (or simulated) material properties and geometry, and with all partial factors set equal to unity.

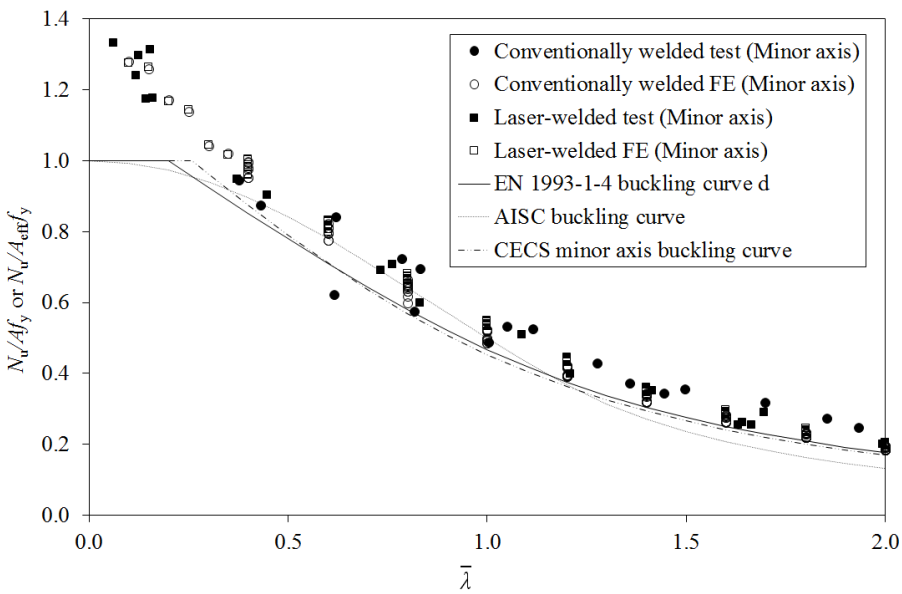

Fig. 4 Comparison of test and FE data with buckling curves for column buckling about the minor axis

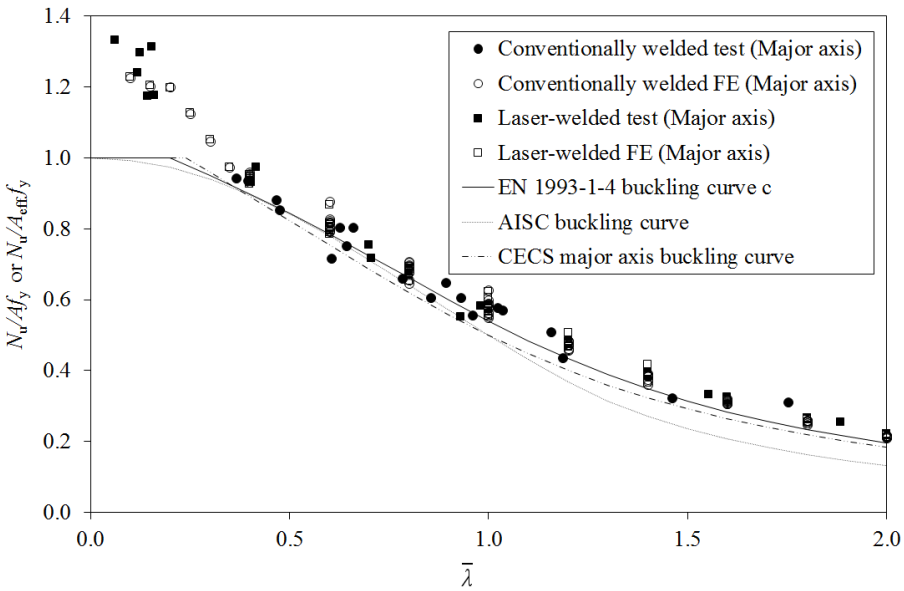

Fig. 5 Comparison of test and FE data with buckling curves for column buckling about the major axis

Table 4 Comparison of experimental and numerical results with EC3, AISC and CECS strength predictions

Welding type	Buckling axis	No. of tests	No. of FE models	N_u/N_{EC3}		N_u/N_{AISC}		N_u/N_{CECS}	
				Mean	COV	Mean	COV	Mean	COV
Conventional welding	Major	19	120	1.06	0.04	1.25	0.20	1.19	0.18
Conventional welding	Minor	18	120	1.10	0.07	1.20	0.17	1.20	0.10
Laser-welding	Major	8	120	1.08	0.05	1.24	0.28	1.17	0.22
Laser-welding	Minor	14	120	1.14	0.03	1.25	0.14	1.24	0.09

In Fig. 6 the ultimate loads from the modelled laser-welded columns $N_{u,lw}$ have been normalised by the ultimate loads of the corresponding conventionally welded columns $N_{u,cw}$ (i.e. the same geometry and material properties but different residual stress distributions) and plotted against the member slenderness. It can be observed that for columns buckling about the major axis, the ratios are close to unity, showing that the residual stress has little effect on the resistance of the column, while for the columns buckling about the minor axis, the laser-welded members exhibit between about 5% and 10% higher resistances, with the greatest difference arising in the intermediate slenderness region, which is known to be the most sensitive to geometric imperfections and residual stresses.

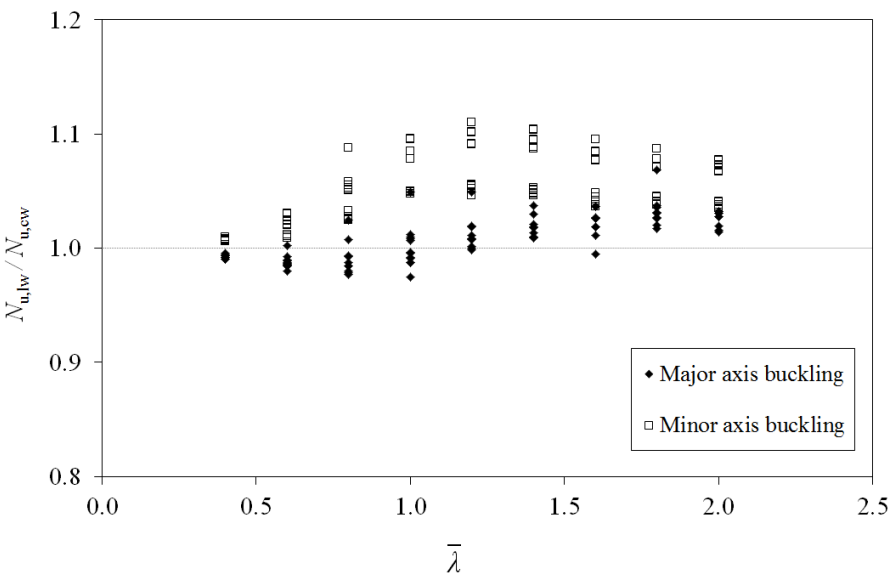

Fig. 6 Comparison of ultimate strength of conventionally welded and laser-welded stainless steel columns

Following the above comparisons and the reliability analysis that is described in Section 4, it is concluded that for both conventionally welded and laser-welded I-section columns buckling about the major axis, the existing EN 1993-1-4 curve is suitable. Adopting the same buckling curve for conventionally welded and laser-welded sections buckling about the major axis is appropriate since the influence of residual stresses for buckling about this axis is relatively small. However, for columns buckling about the minor axis, the influence of residual stress is more significant, and it is recommended that the imperfection factor α is retained at 0.76 for conventionally welded I-section columns, but reduced to 0.60 for laser-welded I-section columns. For all cases, a plateau length $\bar{\lambda}_0$ =0.2 is considered to be suitable. The existing and recommended imperfection factors α and plateau length $\bar{\lambda}_0$ are summarised in Table 5. The existing and proposed buckling curves for conventionally welded and laser-welded stainless steel I-section columns buckling about the minor axis are compared with the test/FE results in Figs. 7 and 8, respectively. The reliability of the proposals is assessed in the following section.

Table 5 Imperfection factors and plateau lengths for EN 1993-1-4 and proposed buckling curves

Welding type	Buckling axis	EN1993-1-4		Proposed	
		α	$\bar{\lambda}_0$	α	$\bar{\lambda}_0$
Conventional welding	Major	0.49	0.20	0.49	0.20
Conventional welding	Minor	0.76	0.20	0.76	0.20
Laser-welding	Major	0.49	0.20	0.49	0.20
Laser-welding	Minor	0.76	0.20	0.60	0.20

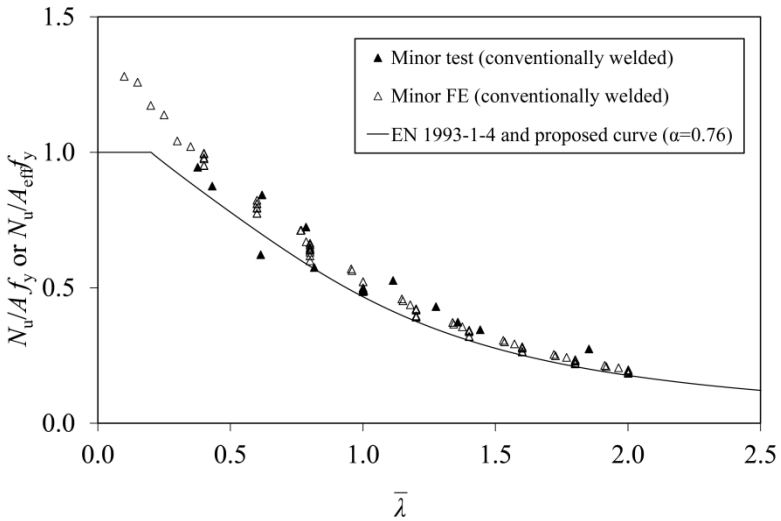

Fig. 7 Existing and proposed buckling curves for conventionally welded stainless steel I-sections buckling about the minor axis

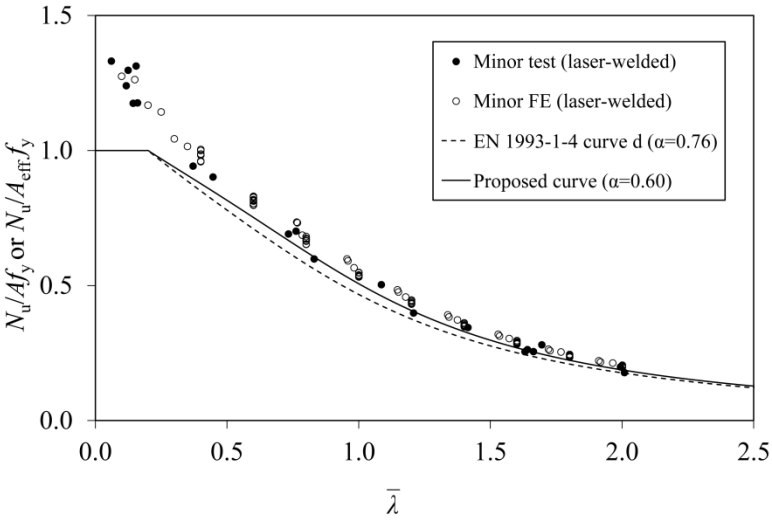

Fig. 8 Existing and proposed buckling curves for laser-welded stainless steel I-sections buckling about the minor axis

4 Reliability Analysis

A reliability study was carried out to assess the applicability and required partial safety factor γ_{M1} of both the existing and proposed buckling curves for welded stainless steel I-section columns on the basis of the experimental and numerical data. The reliability analyses were undertaken initially for non-slender cross-sections (Class 1-3) only, to isolate member buckling behaviour, without the influence of local buckling. The reliability analyses were carried out in accordance with Annex D of EN 1990 [29]. The key statistical parameters are presented in Table 6 for the analysis of the existing EN1993-1-4 buckling curves and Table 7 for the proposed buckling curves, where n is the size of the dataset, *b* is the mean value correction factor, $k_{d,n}$ is the fractile factor and is related to the size of the dataset and V_δ is the coefficient of variation of the test/FE capacities relative to the resistance model. The parameter *b* is taken as the average of the ratios of the test and FE results to predicted resistances; unlike the least squares approach recommended in Annex D, this method does not bias the value of *b* towards results with higher failure loads. The material over-strength factor and the coefficients of variation of the yield strength V_{fy} and geometry $V_{geometry}$ were taken as the values recommended in [30].

Table 6 Summary of reliability analysis results for EN 1993-1-4 buckling curves

Welding type	Buckling axis	Dataset	*n*	*b*	$k_{d,n}$	V_δ	γ_{M1}
Conventional welding	Major	Tests+FE	95	1.06	3.11	0.039	1.02
Conventional welding	Major	Tests only	14	1.01	3.11	0.046	1.08
Conventional welding	Minor	Tests+FE	90	1.09	3.11	0.056	1.04
Conventional welding	Minor	Tests only	12	1.15	3.11	0.120	1.15
Laser-welding	Major	Tests+FE	89	1.09	3.11	0.052	1.04
Laser-welding	Major	Tests only	8	1.14	3.11	0.113	1.11
Laser-welding	Minor	Tests+FE	92	1.14	3.11	0.028	0.95
Laser-welding	Minor	Tests only	14	1.11	3.11	0.051	1.00

Table 7 Summary of reliability analysis results for proposed buckling curves

Welding type	Buckling axis	Dataset	n	b	$k_{d,n}$	V_δ	γ_{M1}
Conventional welding	Major	Tests+FE	95	1.06	3.11	0.039	1.02
Conventional welding	Major	Tests only	14	1.01	3.11	0.046	1.08
Conventional welding	Minor	Tests+FE	90	1.09	3.11	0.056	1.04
Conventional welding	Minor	Tests only	12	1.15	3.11	0.120	1.15
Laser-welding	Major	Tests+FE	89	1.09	3.11	0.052	1.04
Laser-welding	Major	Tests only	8	1.14	3.11	0.113	1.11
Laser-welding	Minor	Tests+FE	92	1.07	3.11	0.029	1.01
Laser-welding	Minor	Tests only	14	1.04	3.11	0.050	1.06

The analyses consistently reveal higher scatter in the resistance predictions (i.e. higher V_δ values) and hence higher required γ_{M1} factors when considering the test data alone than when considering both the test and FE data. The higher scatter is associated with the smaller dataset and the greater inherent variability associated with experimental results. Considering both the test and FE data, the existing EN 1993-1-4 provisions may be seen to be suitable for major axis buckling of both conventionally welded and laser-welded members (i.e. the required γ_{M1} values are close to the target value employed in EN 1993-1-4 of 1.1). It is therefore proposed that the existing buckling curves are retained. For buckling about the minor axis, it is also proposed to retain the existing EN 1993-1-4 buckling curve (α=0.76 and $\bar{\lambda}_0$=0.2) for conventionally welded sections, but there is scope for improvement for laser-welded sections; a higher buckling curve (α=0.60 and $\bar{\lambda}_0$=0.2) for laser-welded columns, which leads to γ_{M1} values closer to the target value of 1.1, is therefore proposed. Having a higher buckling curve for laser-welded columns than conventionally welded columns buckling about the minor axis reflects the improved performance for buckling about this axis arising from the lower residual stress levels.

The proposed curves were also found to be safely applicable to members with Class 4 cross-sections, achieving γ_{M1} values of 1.07, 1.00, 1.08 and 1.04, for conventionally welded columns buckling about the major axis, conventionally welded columns buckling about the minor axis, laser-welded columns buckling about the major axis and laser-welded columns buckling about the minor axis, respectively. It is therefore concluded that the existing buckling curves for conventionally welded I-section columns and new buckling curves for laser-welded I-section columns (given in Table 5) satisfy the Eurocode reliability requirement, and these buckling curves are recommended for inclusion in future revisions of EN 1993-1-4 and other standards.

5 Conclusions

The member buckling behaviour and design of austenitic stainless steel welded I-section columns has been investigated. Finite element models were developed and validated against experimental results obtained from previous studies, covering different stainless steel material types (austenitic and duplex grades), buckling about both axes (the major axis and the minor axis) and different fabrication process (conventional welding and laser-welding). Upon validation of the models, a parametric study of 480 columns with a wide range of member slenderness was carried out. The experimental and numerical results were compared with resistance predictions from current international design standards. Based on the findings, retaining the existing buckling curves for conventionally welded stainless steel I-sections is recommended while, for laser-welded I-section members, new buckling have been proposed for the first time. Reliability analyses were undertaken, which demonstrate that the new buckling curves satisfy the reliability requirements of the Eurocode, in conjunction with a partial safety factor γ_{M1}=1.1; it is recommended that the proposed buckling curves are considered for future revisions of EN 1993-1-4 and other stainless steel design standards.

Acknowledgements

The authors would like to thank Montanstahl AG for the supply of test specimens and financial support for the experimental programme. The financial support provided by the China Scholarship Council for Yidu Bu's PhD study is also gratefully acknowledged.

References

[1] BA Burgan, NR Baddoo, and KA Gilsenan. Structural design of stainless steel members-comparison between Eurocode 3, Part 1.4 and test results. Journal of Constructional Steel Research, 54(1):51–73, 2000.

[2] L Yang, M Zhao, TM Chan, F Shang, and D Xu. Flexural buckling of welded austenitic and duplex stainless steel I-section columns. Journal of Constructional Steel Research, 122:339–353, 2016.

[3] L Gardner, Y Bu, and M Theofanous. Laser-welded stainless steel I-sections: Residual stress measurements and column buckling tests. Engineering Structures, 127:536–548, 2016.

[4] HX Yuan, YQWang, L Gardner, XX Du, and YJ Shi. Local–overall interactive buckling behaviour of welded stainless steel I-section columns. Journal of Constructional Steel Research, 111:75–87, 2015.

[5] HX Yuan, YQ Wang, L Gardner, and YJ Shi. Local–overall interactive buckling of welded stainless steel box section compression members. Engineering Structures, 67:62–76, 2014.

[6] L Yang, M Zhao, D Xu, F Shang, H Yuan, Y Wang, and Y Zhang. Flexural buckling behavior of welded stainless steel box-section columns. Thin-Walled Structures, 104:185–197, 2016.

[7] EN 1993-1-4:2006+A1:2015. Eurocode 3: Design of steel structures - Part 1.4: General rules supplementary rules for stainless steels. European Committee for Standardization (CEN), 2015.

[8] AISC. Design Guide 27: Structural Stainless Steel. Chicago, Illinois, USA, 2013.

[9] CECS-410. Technical Specification for Stainless Steel Structures. China Planning Press, Beijing (in Chinese), 2015.

[10] Y Huang and B Young. Structural performance of cold-formed lean duplex stainless steel columns. Thin-Walled Structures, 83:59–69, 2014.

[11] L Gardner and M Ashraf. Structural design for non-linear metallic materials. Engineering Structures, 28(6):926–934, 2006.

[12] K JR Rasmussen. Full-range stress-strain curves for stainless steel alloys. Journal of Constructional Steel Research, 59(1):47–61, 2003.

[13] E Mirambell and E Real. On the calculation of deflections in structural stainless steel beams: an experimental and numerical investigation. Journal of Constructional Steel Research, 54(1):109–133, 2000.

[14] I Arrayago, E Real, and L Gardner. Description of stress-strain curves for stainless steel alloys. Materials & Design, 87:540–552, 2015.

[15] M Theofanous, TM Chan, and L Gardner. Flexural behaviour of stainless steel oval hollow sections. Thin-Walled Structures, 47(6):776–787, 2009.

[16] J Wang and L Gardner. Flexural buckling of hot-finished high-strength steel SHS and RHS columns. Journal of Structural Engineering (ASCE), 143(6):04017028, 2017.

[17] RG Dawson and AC Walker. Post-buckling of geometrically imperfect plates. Journal of the Structural Division (ASCE), 98(1):75–94, 1972.

[18] L Gardner and DA Nethercot. Numerical modeling of stainless steel structural components - A consistent approach. Journal of Structural Engineering (ASCE), 130(10):1586–1601, 2004.

[19] ABAQUS. ABAQUS/Standard user's manual volumes I-III and ABAQUS CAE manual. Dassault Systemes Simulia Corporation, 2014.

[20] E Riks. An incremental approach to the solution of snapping and buckling problems. International Journal of Solids and Structures, 15(7):529–551, 1979.

[21] O Lagerqvist and A Olsson. Residual stresses in welded I-girders made of stainless steel and structural steel. Proceedings of 9th Nordic Steel Construction Conference, 2001.

[22] PJ Bredenkamp and GJ Van den Berg. The strength of stainless steel built-up I-section columns. Journal of Constructional Steel Research, 34(2):131–144, 1995.

[23] L Gardner and RB Cruise. Modeling of residual stresses in structural stainless steel sections. Journal of Structural Engineering (ASCE), 135(1):42–53, 2009.

[24] JJ Klopper, RF Laubscher, A Steuwer, and MN James. An investigation into the effect of weld technique on the residual stress distribution of 3CR12 (DIN 1.4003) built-up structural sections. Proceedings of the Institution of Mechanical Engineers, Part L: Journal of Materials Design and Applications, 225(3):123–132, 2011.

[25] HX Yuan, YQ Wang, YJ Shi, and L Gardner. Residual stress distributions in welded stainless steel sections. Thin-Walled Structures, 79:38–51, 2014.

[26] ECCS. Manual on stability of steel structures - Part 2.2. Mechanical properties and residual stresses. Brussels, 1976.

[27] BSK99. Swedish regulations for steel structures. Boverket. Karlskrona, Sweden, 2003.

[28] EN 1993-1-5. Eurocode 3: Design of steel structures - Part 1.5: General rules and supplementary rules for plated structures. European Committee for Standardization (CEN), 2006.

[29] EN 1990:2002+A1:2005. Eurocode - Basis of structural design. European Committee for Standardization (CEN), 2005.

[30] S Afshan, P Francis, NR Baddoo, and L Gardner. Reliability analysis of structural stainless steel design provisions. Journal of Constructional Steel Research, 114:293–304, 2015.

